

ROBUST UNSUPERVISED MULTI-OBJECT TRACKING IN NOISY ENVIRONMENTS

C.-H. Huck Yang^{1†}, Mohit Chhabra², Y.-C. Liu¹, Quan Kong², Tomoaki Yoshinaga², Tomokazu Murakami²

¹Georgia Institute of Technology, Atlanta, GA, USA

²Lumada Data Science Lab. Hitachi, Ltd., Tokyo, Japan

ABSTRACT

Camera movement and unpredictable environmental conditions like dust and wind induce noise into video feeds. We observe that popular unsupervised MOT methods are dependent on noise-free conditions. We show that the addition of a small amount of artificial random noise causes a sharp degradation in model performance on benchmark metrics. We resolve this problem by introducing a robust unsupervised multi-object tracking (MOT) model: AttU-Net. The proposed single-head attention model helps limit the negative impact of noise by learning visual representations at different segment scales. AttU-Net shows better unsupervised MOT tracking performance over variational inference-based state-of-the-art baselines. We evaluate our method in the MNIST and the Atari game video benchmark. We also provide two extended video datasets consisting of complex visual patterns that include Kuzushiji characters and fashion images to validate the effectiveness of the proposed method.

Index Terms— Multi-object tracking, unsupervised learning, video tracking, and robust representation learning.

1. INTRODUCTION

Multi-object tracking (MOT) is a challenging video processing task, which aims to locate and track one or more visual pattern(s) from an input video. MOT has many essential real-world applications, such as multimedia content analysis [1, 2, 3] and industrial automation [4, 5]. However, the time and pecuniary cost of labeling large-scale video data constrain the effectiveness of current methods. Unsupervised Multi-Object Tracking (UMOT) is an appealing approach to further improve performance without the requirement of labeling training data for various applications.

Different from the UMOT evaluations of video data in carefully controlled laboratory settings, real-world applications often require data processing in the presence of **environmental noise** as shown in Figure 1. In addition, the robustness of UMOT performance against environmental noise remains relatively unexplored. In this work, we first evaluate the robustness of the state-of-the-art UMOT model against artificial

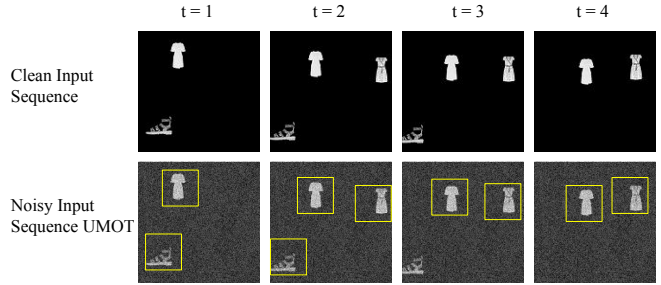


Fig. 1: Unsupervised multi-object tracking (UMOT) on a new fashion context video dataset is motivated by setups in [6, 8].

random noise. We then propose a multi-scale tracker based on attention U-Net to improve model generalization and to avoid over-fitting on irrelevant pixels. Finally, we conduct ablation studies on different visual and optimization setups in the MNIST video benchmark and two extended video datasets. Our contributions include:

- Investigate the effect of noise on UMOT performance.
- Propose a new DNN video tracking backbone to leverage upon attention U-Net for robust UMOT and attain competitive results.
- Evaluate the proposed method in the MNIST video [6], Atari gaming video [7], and two newly created UMOT datasets with complex patterns: (1) Japanese cursive characters (Kuzushiji) and (2) fashion images.

2. RELATED WORK

2.1. Unsupervised Multi-Object Tracking

Unsupervised learning based object tracking often incorporates visual reconstruction and geometric rendering to use spatial information for predicting bounding boxes. Tracking by animation [6] (TBA) showed the first competitive UMOT results on both the MNIST video and DukeMTMC [9] dataset. It used a recurrent neural network (RNN) to learn the representations of object motions and a convolutional neural network (CNN) based autoencoder to reconstruct frames and visual patterns from geometrical tracker arrays. Spatially invariant attend-infer-repeat (SPAIR) models [8] used

[†]Parts of work are finished during Huck's visiting at Hitachi Central Research Lab, Tokyo, Japan.

CNN feature extractors and a local spatial object specification scheme to conduct UMOT video processing with variational inference. Building upon the SPAIR method, spatially invariant label-free object tracking (SILOT) [7] incorporated VAE based architecture with competitive MOT accuracy on MNIST video and Atari video games. However, the previous methods and benchmark models do not provide experimental studies on the effect of background noise on tracker performance. This motivates the evaluation setup under noisy conditions presented in this work.

2.2. Self attention for robustness

Image denoising [10, 11, 12] with the objective of image enhancement has been studied extensively in the literature (e.g., image dehazing [13]). Image denoising approaches have also been investigated in the context of improving representation learning. U-Net [14, 15] was initially introduced for the task of biomedical image segmentation with few labeled images. U-Net based multi-scale learning architectures, such as Wave-U-Net [16] and attention U-Nets [17, 18], have attained competitive results against the noisy inputs by learning across multiple scales over input segments. Recently, Siam-U-Net [19] has also shown that U-Net based encoders with competitive performance on visual tracking. In this work, we build upon U-Net based backbone for UMOT with the motivation of enhancing model generalization with multi-scale denoising.

3. ENHANCED UNSUPERVISED MULTI-OBJECT TRACKING

3.1. Noisy Background Setup

For reproducible studies, we first define a loss objective l_t at time t in a standard setup UMOT model, TBA (refer to Eq. (9) in [6]):

$$l_t = \text{MSE}(\mathbf{X}_t, \mathbf{X}_t^C) + \lambda \cdot \frac{1}{I} \sum_{i=1}^4 (s_{t,i}^x, s_{t,i}^y), \quad (1)$$

where the first term is the reconstruction mean squared error (MSE) between \mathbf{X}_t (a grounded truth frame) and \mathbf{X}_t^C (generated by DNN reconstruction), and the second term is tightness constraint on the bounding boxe size computed by λ (a scaling coefficient), I (a number of trackers), and $s_{t,i}^x, s_{t,i}^y$ (object poses).

To simulate remaining environment noise received from the image sensors, we consider a random noise $\delta_t \sim \mathcal{N}(0, 1)$ sampled from Gaussian distribution, which has been used in robust video learning studies [20, 21, 4]. The total training frames of a video input in Eq. (1) are modified to $\sum_{t=1}^T \mathbf{X}'_t = \sum_{t=1}^T (\mathbf{X}_t + \beta \times \delta_t)$ as a **noisy setup in testing** for total time step $t \in \{1, 2, \dots, T\}$, where

$\beta \in \{0\%, 10\%, 20\%, 30\%\}$ refers to a noise ratio (level) with a maximum threshold of 30% refer to [21, 20].

3.2. Attention U-Net Feature Encoder

We first design a spatial feature encoder consisting of transformer-based single-head attention [22, 23] (A_t) is computed by a feature map (m_t) with a ResNet₁₈ [24] encoder extracting from \mathbf{X}_t feeding into keys (k_t) and value (v_t) with queries (q_t):

$$m_t = f_{\text{ResNet}, \theta_1}(\mathbf{X}_t); \quad q_t = \text{unroll}(f_{q, \theta_2}(m_t)); \quad (2)$$

$$k_t = \text{unroll}(f_{k, \theta_3}(m_t)); \quad v_t = \text{unroll}(f_{v, \theta_4}(m_t)); \quad (3)$$

$$A_t = \text{softmax} \left(\frac{q_t k_t^T}{\sqrt{d_k}} \right) v_t, \quad (4)$$

where f_{ResNet} , f_q , f_k , f_v are individual DNNs with hyper-parameters (θ_1 to θ_4) updated by end-to-end gradient descent training.

As shown in Figure 2 (a), a U-Net [14] encoder is further introduced to learn multi-scale features from the attention map $C_t = \text{U-Net}(A_t; \theta_5)$. The attention U-Net comprises of channel sizes $\{32, 64, 128, 64, 32\}$. Each step followed by a rectified linear unit and a 2×2 max-pooling operation with stride 2 for down-sampling.

3.3. Tracker Arrays and Rendering

After attaining the feature representation C_t , we use tracker arrays to extract the individual location of the object(s) from a frame. As shown in Figure 2 (b), we use a latent state $\mathbf{H}_{(t,i)}$ feature extractor for i -th tracker to convert spatial information by neural sequence modeling:

$$\mathbf{H}_{(t,i)} = f_{\text{seq}, \theta_6}(\mathbf{H}_{t-1}, C_t), \quad (5)$$

where f_{seq, θ_6} consists of bidirectional GRU [25] networks. To obtain the location of objects in the unsupervised manner, we incentivize each tracker network to predict a single object location ($\mathbf{Y}_{t,i}$) from joint parameterized network (f_{joint}) shared by all trackers:

$$\mathbf{Y}_{t,i} = f_{\text{joint}}(\mathbf{h}_{t,i}; \theta^{\text{out}}) \quad (6)$$

where the output $\mathbf{Y}_{t,i}$ is a mid-level representation of objects on 2D image planes, including: (a) probability of having tracked an object; (b) object pose ($s_{t,i}^x, s_{t,i}^y$ in Eq. (1)); (c) shape (with channel size); (d) object appearance. These mid-level output locations will be used to validate model performance by MOT evaluation. Next, we follow the layer-wise composition setup from TBA [6] and use Spatial Transformer Network (STN) [26] to scale $\mathbf{Y}_{t,i}$ to multiple layer foreground (L_t^k) and layer masks ($L-m_t^k$) with layer number

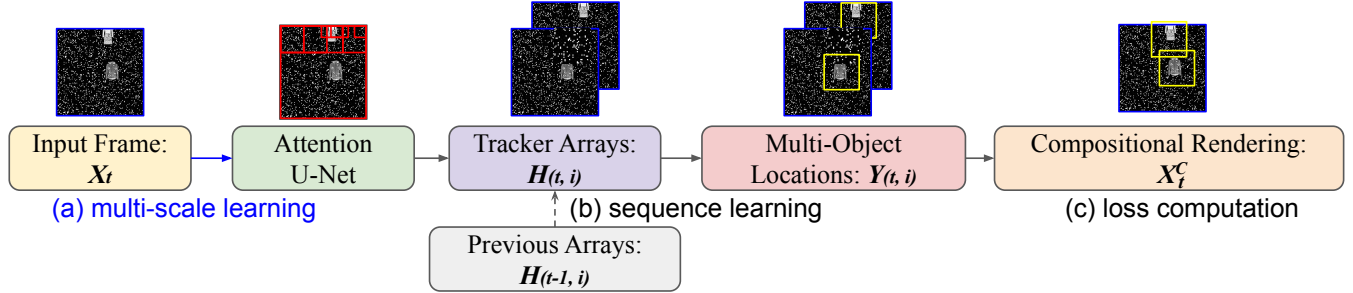


Fig. 2: Overview of the U-Net enhanced animation tracking frame-work: (a) multi-scale learning; (b) sequence learning; (c) loss computation.

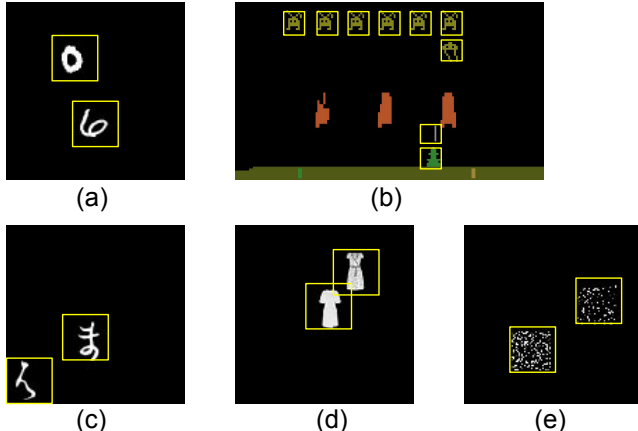


Fig. 3: Four training datasets used in our experiments: (a) MNIST video [6, 8], (b) Atari gaming video [7], (c) Kuzushiji video, and (d) Fashion video. A test dataset with scrambled objects (e) is provided to evaluate context learning effects.

$k = 3$. As shown in Figure 2 (c), we contain the DNN reconstructed frame \mathbf{X}_t^C by using layer-wise geometrical composition:

$$\mathbf{X}_t^{(k)} = (\mathbf{1} - L \cdot m_t^k) \odot \mathbf{X}_t^{(k-1)} + L_t^k; \quad (7)$$

$$\mathbf{X}_t^C = \sum_{k=1}^3 \mathbf{X}_t^{(k)}, \quad (8)$$

where \mathbf{X}_t^C is used in the reconstruction loss computation in Eq. (1).

4. EXPERIMENT

4.1. Dataset and Baseline Setup

As shown in Figure 3, we select two baseline video dataset settings from the previous UMOT studies: (a) MNIST MOT video [6, 8] containing $2M$ training frames and $25k$ validation frames, where each frame is of size $128 \times 128 \times 1$ and (b) Atari gaming video on Space-Invader (Atari-SI) [7, 8] containing $128k$ training frames and $1k$ validation frames, where each frame is converted to Gray-scale with a input size of $210 \times 160 \times 1$ for testing.

MOT Video Datasets: To study the effects of tracking on different visual patterns beyond MNIST-video, we further provide two new MOT video datasets with more intricate context patterns included (c) Japanese cursive characters (denoted as **Kuzushiji** from [27]) and (d) fashion clothes images (denoted as **Fashion** from [28]). These new data datasets aim to study complex visual patterns and could be useful for different UMOT applications (e.g., clothes tracking).

Object-Scrambling Test: To verify whether the unsupervised model learns indeed learns the context-patterns, we provide an **object-scrambling** testing video dataset containing $1k$ frames as (e) in Figure 3 modified from the MNIST-video, which makes random scrambling inside the object bounding boxes. Ideally, a robust UMOT model [8, 4] should learn consistent discriminative representations to predict object locations, this would indicate the usefulness of Att-U-Net in improving robustness. On context-wise MNIST video dataset – a model which learns consistent discriminative patterns would have degraded performance on test set.

Baseline Models: We select two major benchmark UMOT models as reproducible studies as shown in Table 1.

- **Tracking by animation (TBA)** [6]: a model combines with RNNs for sequence modeling with attention features and uses CNN feature extraction for representation learning on frame rendering.
- **Spatially invariant label-free object tracking (SILOT)** [7]: a model built upon VAE for frame-wise reconstruction and using YOLO-based CNN feature extraction for representation learning.

U-Net based UMOT backbones: We design two different type of U-Net based feature encoder backbones: residual network U-Net with a ResNet₅₀ encoder (denoted as **ResU-Net**) and proposed self-attention U-Net (denoted as **AttU-Net**) as discussed in section 3.2.

The tested UMOT models have a similar $\sim 12M$ parameters regrading to the model capacity in our experiment.

4.2. UMOT Performance in Different Contexts

We first evaluate the MOT accuracy as shown in Figure 4 with noise level ranging from 0% (without noise) to 30%. All

Table 1: Detailed MOT metrics in the clean MNIST video [6, 7] with UMOT models as a reproducible baseline.

Model	IDF1	IDP	IDR	Rcll	Prcn	GT	MT	PT	ML	FP	FN	IDs	FM	MOTA	MOTP
TBA	99.4%	99.3%	99.5%	99.8%	99.6%	99	99	2	0	9	4	2	1	99.3%	88.4%
SILOT	98.9%	98.2%	99.5%	99.9%	98.5%	100	100	0	0	34	3	7	1	98.0%	85.9%
ResU-Net	99.5%	99.5%	99.8%	100.0%	99.7%	99	99	0	4	3	2	1	0	99.4%	89.2%
AttU-Net	99.9%	99.9%	100.0%	100.0%	99.9%	99	99	0	0	3	1	1	0	99.8%	89.6%

the models were trained with clean video frames as shown in Figure 3 (a) to (d). In the clean settings (0%), MNIST (4a) and Kuzushiji (4c) video dataset are less challenging when all the model could attain ~ 95 to 99% MOT accuracy; Atari-SI (4b) and Fashion (4d) are much competitive for context-wise learning where the models could only attain MOT accuracy below 90%. As the noise magnitude increases, TBA models show a sharp decrease in MOT accuracy over all tested datasets and it falls below $\sim 20\%$ in the MNIST dataset.

Although SILOT models are more robust than TBA under the presence of small amount of noise. Their performance suffers major degradation when the noise ratio is increased. It decreases to 52.12% in Atari-SI when the noise level is 20%. For U-Net based backbones, both ResU-Net and AttU-Net show a robustness in the MNIST dataset even with the presence 30% noise. Over all context-wise datasets, AttU-Net based UMOTs show best performance with significant absolute improvements ($\sim 3\text{-}5\%$) from the ResU-Net excluded Fashion (1.01%) as (4d). In conclusion, the performance of existing benchmark UMOTs, TBA and SILOT, are sensitive to the noise whereas U-Net based UMOTs show competitive results.

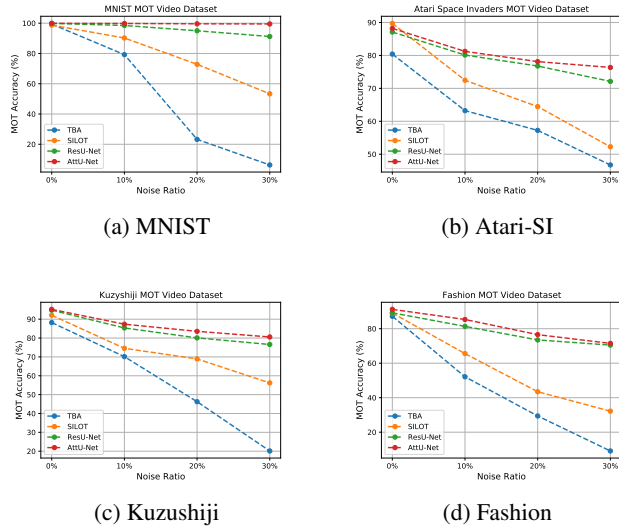


Fig. 4: MOTA Performance under different noisy level testing in: (a) MNIST video [8, 6], (b) Atari-Space Invader [7] (SI) video, (c) Kuzushiji video, and (d) Fashion video tracking datasets.

4.3. Evaluation of UMOT Model Generalization

To study generalization of different UMOT models with noisy inputs, we evaluate pre-trained UMOT models on MNIST video test set in two different configurations.

(1) Testing with scrambled objects: As in Table 2, U-Net backbones show major degradation when context-wise representation has been corrupted by the scrambled object settings (S). As discussed in Section 4.1 U-Net backbones generalize better than baseline models.

(2) Training with augmented noise: We also evaluate as to how models would benefit from training with noisy Fashion dataset. As shown in Table 3, both U-Net based UMOT models show better performance than TBA and SILOT by a noisy training (N) with augmented inputs containing 30% noise ratio. All UMOTs improve in terms of absolute performance but the architecture-specific (e.g., multi-scale learning by U-Net based backbones) differences still significantly impact performance metrics.

Table 2: Performance (\downarrow) of pretrained UMOT models in MNIST but testing with the scrambled MNIST objects (S).

	TBA [6]	SILOT [7]	ResU-Net	AttU-Net
<i>S</i> -MOTA	91.4%	83.9%	65.1%	61.7%
<i>S</i> -MOTP	90.9%	82.1%	61.4%	59.8%

Table 3: Performance (\uparrow) of different UMOT models trained with a 30% noise (N) in Fashion video dataset.

	TBA [6]	SILOT [7]	ResU-Net	AttU-Net
<i>N</i> -MOTA	24.1%	46.7%	76.3%	81.2%
<i>N</i> -MOTP	23.2%	44.8%	75.2%	80.1%

5. CONCLUSION

In this work, we studied UMOT performance under the influence of input noise and show that pre-existing methods suffer a significant decrease in MOT accuracy when the noise ratio is increased above 30%. AttU-Net based approach increases the robustness of all tested data sets. We show the capability of AttU-Net to useful learn discriminative features by testing it on the test set of scrambled instances. In future work, we plan to incorporate more latent training studies [29], low-complexity single stream module [30] and investigate additive noise [31, 32] (e.g., deferentially private) effects for UMOT.

6. REFERENCES

- [1] Anders Johansson, Dirk Helbing, and Pradyumn K Shukla, “Specification of the social force pedestrian model by evolutionary adjustment to video tracking data,” *Advances in complex systems*, vol. 10, no. supp02, pp. 271–288, 2007.
- [2] Jia-Hong Huang and Marcel Worring, “Query-controllable video summarization,” in *Proceedings of the 2020 International Conference on Multimedia Retrieval*, 2020, pp. 242–250.
- [3] Jia-Hong Huang, Ting-Wei Wu, and Marcel Worring, “Contextualized keyword representations for multi-modal retinal image captioning,” *arXiv preprint arXiv:2104.12471*, 2021.
- [4] Sorin Grigorescu, Bogdan Trasnea, Tiberiu Cocias, and Gigel Macesanu, “A survey of deep learning techniques for autonomous driving,” *Journal of Field Robotics*, vol. 37, no. 3, pp. 362–386, 2020.
- [5] Jia-Hong Huang, Luka Murn, Marta Mrak, and Marcel Worring, “Gpt2mvs: Generative pre-trained transformer-2 for multi-modal video summarization,” *arXiv preprint arXiv:2104.12465*, 2021.
- [6] Zhen He, Jian Li, Daxue Liu, Hangen He, and David Barber, “Tracking by animation: Unsupervised learning of multi-object attentive trackers,” in *Proceedings of the IEEE Conference on Computer Vision and Pattern Recognition*, 2019, pp. 1318–1327.
- [7] Eric Crawford and Joelle Pineau, “Exploiting spatial invariance for scalable unsupervised object tracking,” in *Proceedings of the AAAI Conference on Artificial Intelligence*, 2020, vol. 34, pp. 3684–3692.
- [8] Eric Crawford and Joelle Pineau, “Spatially invariant unsupervised object detection with convolutional neural networks,” in *Proceedings of the AAAI Conference on Artificial Intelligence*, 2019, vol. 33, pp. 3412–3420.
- [9] Mengran Gou and et al., “Dukemtmc4reid: A large-scale multi-camera person re-identification dataset,” in *Proc. CVPR Workshops*, 2017, pp. 10–19.
- [10] Antoni Buades, Bartomeu Coll, and Jean-Michel Morel, “A review of image denoising algorithms, with a new one,” *Multiscale Modeling & Simulation*, vol. 4, no. 2, pp. 490–530, 2005.
- [11] Hao-Hsiang Yang, Kuan-Chih Huang, and Wei-Ting Chen, “Laffnet: A lightweight adaptive feature fusion network for underwater image enhancement,” *arXiv preprint arXiv:2105.01299*, 2021.
- [12] Hao-Hsiang Yang, Wei-Ting Chen, Hao-Lun Luo, and Sy-Yen Kuo, “Multi-modal bifurcated network for depth guided image relighting,” *arXiv preprint arXiv:2105.00690*, 2021.
- [13] Hao-Hsiang Yang, Chao-Han Huck Yang, and Yi-Chang James Tsai, “Y-net: Multi-scale feature aggregation network with wavelet structure similarity loss function for single image dehazing,” in *2020 IEEE International Conference on Acoustics, Speech and Signal Processing (ICASSP)*. IEEE, 2020, pp. 2628–2632.
- [14] Olaf Ronneberger, Philipp Fischer, and Thomas Brox, “U-net: Convolutional networks for biomedical image segmentation,” in *International Conference on Medical image computing and computer-assisted intervention*. Springer, 2015, pp. 234–241.
- [15] C-H Huck Yang, Jia-Hong Huang, Fangyu Liu, Fang-Yi Chiu, Mengya Gao, Weifeng Lyu, Jesper Tegner, et al., “A novel hybrid machine learning model for auto-classification of retinal diseases,” *arXiv preprint arXiv:1806.06423*, 2018.
- [16] Hao-Hsiang Yang and Yanwei Fu, “Wavelet u-net and the chromatic adaptation transform for single image dehazing,” in *2019 IEEE International Conference on Image Processing (ICIP)*. IEEE, 2019, pp. 2736–2740.
- [17] Ozan Oktay and et al., “Attention u-net: Learning where to look for the pancreas,” *arXiv preprint arXiv:1804.03999*, 2018.
- [18] Hao-Hsiang Yang, Chao-Han Huck Yang, and Yu-Chiang Frank Wang, “Wavelet channel attention module with a fusion network for single image deraining,” in *2020 IEEE International Conference on Image Processing (ICIP)*. IEEE, 2020, pp. 883–887.
- [19] Matteo et al. Dunnhofer, “Siam-u-net: encoder-decoder siamese network for knee cartilage tracking in ultrasound images,” *Medical Image Analysis*, vol. 60, pp. 101631, 2020.
- [20] Chao-Han Huck Yang, Jun Qi, Pin-Yu Chen, Yi Ouyang, I-Te Danny Hung, Chin-Hui Lee, and Xiaoli Ma, “Enhanced adversarial strategically-timed attacks against deep reinforcement learning,” in *2020 IEEE International Conference on Acoustics, Speech and Signal Processing (ICASSP)*. IEEE, 2020, pp. 3407–3411.
- [21] Yen-Chen Lin and et al., “Tactics of adversarial attack on deep reinforcement learning agents,” in *Proceedings of the 26th International Joint Conference on Artificial Intelligence*, 2017, pp. 3756–3762.

- [22] Chao-Han Yang, Jun Qi, Pin-Yu Chen, Xiaoli Ma, and Chin-Hui Lee, “Characterizing speech adversarial examples using self-attention u-net enhancement,” in *2020 IEEE International Conference on Acoustics, Speech and Signal Processing (ICASSP)*. IEEE, 2020, pp. 3107–3111.
- [23] Ashish Vaswani and et al., “Attention is all you need,” *Advances in Neural Information Processing Systems*, vol. 30, pp. 5998–6008, 2017.
- [24] Kaiming He, Xiangyu Zhang, Shaoqing Ren, and Jian Sun, “Deep residual learning for image recognition,” in *Proceedings of the IEEE conference on computer vision and pattern recognition*, 2016, pp. 770–778.
- [25] Junyoung Chung, Caglar Gulcehre, KyungHyun Cho, and Yoshua Bengio, “Empirical evaluation of gated recurrent neural networks on sequence modeling,” *arXiv preprint arXiv:1412.3555*, 2014.
- [26] Max Jaderberg, Karen Simonyan, Andrew Zisserman, et al., “Spatial transformer networks,” *Advances in neural information processing systems*, vol. 28, pp. 2017–2025, 2015.
- [27] Tarin Clanuwat and et al., “Deep learning for classical japanese literature,” *arXiv preprint arXiv:1812.01718*, 2018.
- [28] Han Xiao and et al., “Fashion-mnist: a novel image dataset for benchmarking machine learning algorithms,” *arXiv preprint arXiv:1708.07747*, 2017.
- [29] Jean-Yves Franceschi, Edouard Delasalles, Mickaël Chen, Sylvain Lamprier, and Patrick Gallinari, “Stochastic latent residual video prediction,” in *International Conference on Machine Learning*. PMLR, 2020, pp. 3233–3246.
- [30] Hao-Hsiang Yang, Wei-Ting Chen, et al., “S3net: A single stream structure for depth guided image relighting,” *arXiv preprint arXiv:2105.00681*, 2021.
- [31] Chao-Han Huck Yang, Sabato Marco Siniscalchi, and Chin-Hui Lee, “Pate-aae: Incorporating adversarial autoencoder into private aggregation of teacher ensembles for spoken command classification,” *arXiv preprint arXiv:2104.01271*, 2021.
- [32] Jia-Hong Huang, Cuong Duc Dao, Modar Alfadly, C Huck Yang, and Bernard Ghanem, “Robustness analysis of visual qa models by basic questions,” *arXiv preprint arXiv:1709.04625*, 2017.